IEEE Access
Multidisciplinary | Rapid Review | Open Access Journal

Received June 24, 2020, accepted July 1, 2020, date of publication July 9, 2020, date of current version July 22, 2020.

Digital Object Identifier 10.1109/ACCESS.2020.3008165

Using EEG and Deep Learning to Predict Motion Sickness Under Wearing a Virtual Reality Device

CHUNG-YEN LIAO[1], (Member, IEEE), SHAO-KUO TAI[1], RUNG-CHING CHEN[1], (Member, IEEE), AND HENDRY HENDRY[2]

[1]Department of Information Management, Chaoyang University of Technology, Taichung 41349, Taiwan
[2]Faculty of Information Technology, Satya Wacana Christian University, Salatiga 50711, Indonesia

Corresponding author: Rung-Ching Chen (crching@cyut.edu.tw)

This work was supported by the Ministry of Science and Technology, Taiwan, under Project MOST-107-2221-E-324-018-MY2.

ABSTRACT Virtual Reality (VR) research has been widely applied in many fields. VR promises to deliver the experience that is beyond the user's imagination. One of the advantages of VR is the feeling it gives of being there. VR can provide experiences impossible in the real world, such as flying, diving in deep water, exploring outer space, or living with dinosaurs. Despite the improvements in the software and hardware, the problem of motion sickness remains. We implement a deep learning model to train and predict motion sickness. A questionnaire is a well-known method to measure motion sickness. The weakness of the questionnaire is the measurement carried out after the user experiences motion sickness symptoms. By using the deep learning and EEG, the system will learn and classify motion sickness. The system learns the user's EEG pattern when they begin to feel the sickness symptoms. The system will be trained using deep learning to identify the sickness patterns in the future. By the EEG patterns, the system can predict the sickness symptoms before it occurs. Our model outperforms traditional models in loss values, accuracy, and F-measure metrics in Roller Coaster. With other datasets, our model also performs well. Our model can achieve 82.83% accuracy from the dataset. We also found that the time steps to predict motion sickness during 5 minute periods is a suitable configuration.

INDEX TERMS Brainwaves EEG, cybersickness, deep learning, motion dizziness detection.

I. INTRODUCTION

Research of Virtual Reality (VR) has been widely applied in many fields. VR is a computer-based environment in which the user can feel their relationship with the environment resembles a real-world experience [1]. Research in VR has been defined as I3: Immersion, 17 Interaction and Imagination. VR promises to deliver experiences beyond human imagination. One of the advantages of using VR is that it creates a feeling of being there. VR tools can generate realistic images, sounds, videos, and other sensory input which replicates the real environment in a digital environment. VR offers the user experiences impossible in real world, such as flying, diving in deep water, exploring outer space, or living with dinosaurs. Beginning in the 1980s, the process of digitally simulating a users' sensory environment gained the term ''Virtual Reality' [2]. A popular application for VR environments is gaming. Early attempts to implement VR in game environments occurred in the 1990s. Sega VR and Nintendo's Virtual Boy are examples of early attempts to mass market VR headsets. They were failures. The limitations of graphics and imprecise controls contributed to an underwhelming experience. Nintendo's headset lasted only a year, while Sega's headset never reached the market. In 2010, VR make a convincing comeback with many big companies, including Oculus Rift, HTC Vive, Sony Playstation VR, and Samsung Gear VR. Although VR has morphed from its original concept, the promise of simulating the real world remains the greatest challenge to scientists and artists [3]. Many improvements have been proposed to enhance the capabilities of VR headsets. Despite the many improvements in the software and hardware, one problem which has not gone away is motion sickness [4].

Motion sickness in VR systems, according to [5], can occur after playing the game for only 17 minutes. A minimum of 59% of participants reported feeling the motion sickness in [5]. Enabling VR to reach its potential, will largely depend on our ability to solve the substantial and enduring problem of motion sickness, which can lead to nausea, dizziness, disorientation, fatigue, and instability. The major cause of motion

The associate editor coordinating the review of this manuscript and approving it for publication was Ahmed A. Zaki Diab.

sickness is undesirable outcomes of hardware and software insufficiency, including low resolution and refresh rates of the image, non-ergonomic interactions, and inappropriate navigation modes [6]–[8]. A common tool for measuring motion sickness in VR is the Simulator Sickness Questionnaire (SSQ). Motion sickness is generally detected after the symptoms appear. This means that the sickness has occurred and the user already feels uncomfortable from its effects.

The development of the electroencephalogram (EEG) enables measurement of many effects of VR. An EEG can be used to measure the cognitive learning which takes place in the VR world. Using an EEG, the system can actively measure the cognitive state of the user, unlike the Brain Computer Interface (BCI) which is commonly used to measure the cognitive state [9]. Use of an EEG with VR enables study of language processing in a naturalistic environment [10]. The learning process occurs by providing words that are appropriate and inappropriate based on the visual context. This will create a situation in which the auditory information is mismatched with what the user sees. In field of emotion detection, an EEG may be used to evaluate the regulation strategies during VR exposure [11]. EEG signals captured from individuals navigating in a virtual environment designed to induce a negative mood will be compared between three experimental groups that receive different instructions about which emotional regulation strategies to apply.

EEG in deep learning has been applied in many fields. Deep learning enables practical machine learning and extension of the overall field of Artificial Intelligence (AI). Making use of EEG data, researchers have proposed methodologies for machine learning and AI research field application. EEG data use and deep learning have been proposed for fields such as classification [12]–[14], clustering [15], recommendation systems [16], [17], health and medication [18], and education [19].

Deep learning is well known for its capability to exploit deep, complex data with multivariate structure. Used in many fields, it is usually applied via neural networks across a wide range of fields. Deep learning works by learning higher-order interactions among features using a cascade of many layers. The core of the deep learning is fast, powerful computers and sufficient data to actually train a large neural network. The difference between deep learning and other learning models is that deep learning performance increases as the amount of data increases, whereas other learning models eventually reach a performance plateau. The capabilities of deep learning systems are continuing to evolve. Fields such as speech and image recognition are developing rapidly. More powerful deep learning systems are under development to assist in VR. In VR, deep learning has been implemented for hand and eye movement tracking and recognition processes.

In this paper, we propose an alternative method for detecting motion sickness in VR headset users that uses an EEG instead of a questionnaire. The main contributions of this paper are: (1) We propose a novel and robust method to detect motion sickness in a VR environment via brainwaves using an EEG and deep learning; (2) we explore user feedback when the user experiences motion sickness from a VR system. We explore how to match the EEG wave with the user's physiology markers; and (3) we predict motion sickness before it occurs based on the user's EEG data.

The remainder of this paper is organized as follows. Section 2 describes previous work on brainwaves, deep learning, and motion sickness detection. Section 3 describes our proposed methodology. Section 4 presents the dataset and the training environment of the system. Section 5 provides the training and testing results of the system. Section 6 offers the conclusions of this paper.

II. LITERATURE REVIEW

A. BRAINWAVES EEG

EEG is emitted from the human brain in the form of a spectrum of frequencies. Each individual emits brainwaves at different frequencies, resulting in different EEG recordings. EEG is very dependent on the activity being carried out. Brainwaves are described as a common fundamental wave in the form of frequency band divisions, and different types of brainwaves reflect the brain's mental state [20]. Brainwaves are classified into five types of waves [21], [22]: Alpha (α), Beta (β), Theta (θ), Delta (δ), and Gamma (γ). Figure 1 shows the frequency range of these brainwaves.

Based on the frequency range, brainwaves are classified into five categories: (1) Delta activity (δ wave) with a frequency below 3 Hz and an amplitude of about 20-200μV. Delta waves usually occur when sleeping or under deep anesthesia or hypoxia, or with brain lesions in patients. (2) Theta activity (θ wave): Between 4 Hz and 7 Hz. In general, it presents a smaller amplitude. Theta waves primarily occur in the top and temporal lobes of children. When adults are under emotional pressure, a small number of Theta waves will appear. However, there is no regular type, and they may occur in a sleepy or highly relaxed state. Analysis of Theta waves is important because many brain diseases are indicated by this wave. (3) Alpha activity (α wave) has a frequency of 8-13 Hz and an amplitude of 20-200μV. In most people, the Alpha wave is generated in a sober, quiet, and relaxed state. To improve Alpha wave activities, people need to close their eyes and feel relaxed. (4) Beta activity (β wave) has a frequency of 13 Hz or more, but is rarely higher than 30 Hz. Studies have shown that Beta waves are influenced by tactile, auditory, and emotional stimuli and can be controlled by self-effort. (5) Gamma activity (γ wave) has a frequency between 31 and 50 Hz. In recent years, researchers have found that this wave is related to the user's attention, awareness, happiness, and reduced stress. Meditation has a connection with human cognition and perceptual activity related to gamma waves [24].

B. MOTION SICKNESS DETECTION

Motion sickness is any sickness produced by motion. In VR, motion sickness is produced by visual motion,

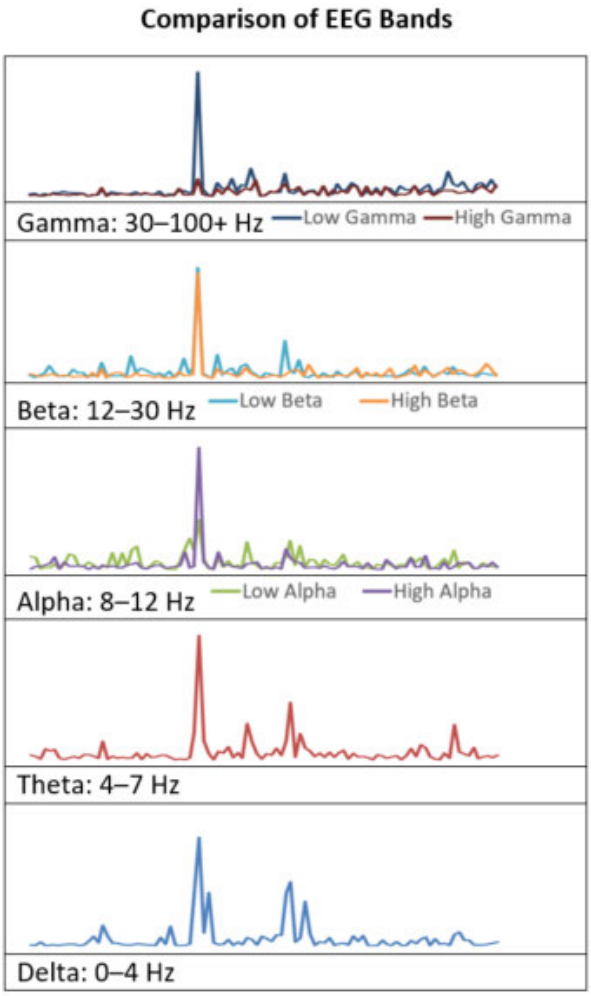

FIGURE 1. The waveform of the Brainwaves EEG [23].

vehicle motion, and other motions. Such motion sickness is termed Cyber-Sickness (CS) [25]. CS is a constellation of symptoms of discomfort and malaise produced by VR exposure [26]. Much research has explored CS [4], [27], [28]. CS is typically categorized as visually induced motion sickness, a distinct sickness produced by observation of visual motion. The symptoms of CS are similar to seasickness or vehicle sickness. While many VR's user experience CS in using the headset, some users appear to be unaffected by CS symptoms. The causal factors of the symptoms have been discussed in many kinds of research. These include such factors as mismatches between observed and expected sensory signals [28], self-motion [29], visual display characteristics [30], and the gameplay experience [31], [32].

CS recently can be measured by objective and subjective measurements. Objective measures are obtained by analysis of physiological markers. For example, increasing gastric activity, respiration rate [33], [34], heart rate [35], and skin conductance at the forehead [36], [37]. All methods reported can provide a robust measurement. Some researchers have proposed behavioral measurements for CS, including early termination [38] and task competence [35], [39]. Another way to measure CS is to use a subjective measurement. Questionnaires are often used to detect CS in VR [40]–[44]. In questionnaires, CS is commonly measured by eyestrain, dizziness, and headache. A 4-point scale is used, with 1 = none, 2 = slight, 3 = moderate, and 4 = severe. CS is then measured by summing up the total sickness score as well as scores for each sub-scale of oculomotor discomfort, disorientation, and nausea.

The challenge of cybersickness detection is how to determine when the user feels symptoms. Previous works have a similarity in detecting cybersickness after the user feels the symptoms. This is due to a detection tool using a questionnaire. The questionnaire was filled out after the user felt symptoms of sickness, or the user did not feel it at all. This study aims to solve this challenge. Using EEG and deep learning, the system learns the series of patterns when the user starts to feel the sickness symptoms.

Table 1 shows the differences with the previous research. The commonly used detection method of cybersickness is by using observation, while the common use of the measurement method of cybersickness is by using a questionnaire. In [34], the author using VR termination to measure the cybersickness. The users will use VR headset until they willingly to stop it by themselves. All the previous research only can predict the cybersickness after the user feels the symptoms, whether they fill the questionnaire or do the VR termination. The difference from the limitation of the previous research, we proposed EEG patterns detection using deep learning LSTM classification model to predict the time before the user starts to feels the symptoms of cybersickness.

TABLE 1. The differences with the previous research.

Reference /Study	Measurement Method	Detection Method	Predict time of CS
França et.al. [6].	Questionnaire	Observation	No
Palmisano et.al. [7]	Questionnaire	Observation	No
Kourtesis et.al. [8]	Questionnaire	Observation	No
Kim et.al. [33]	Questionnaire	Respiration Rate	No
Dennison et.al. [34]	VR Termination	Linear Discriminant Analysis	No
Nalivaiko et.al. [35]	Heart Rate	Parrot Coaster and Helix	No
	Questionnaire	CNN	No
Proposed Method	EEG Patterns	Deep Learning LSTM	Yes

III. PROPOSED METHODOLOGY

In this section, we describe our proposed methodology to detect motion sickness in a VR environment. The VR headset we use is the HTC Vive. Figure 3 shows the system architecture. The system consists of three main steps. First is EEG data collection, second is EEG data analysis and classification, and the final step is using the deep learning model to predict the motion sickness. EEG data is recorded using a Neurosky Mindwave Mobile. This headset uses single

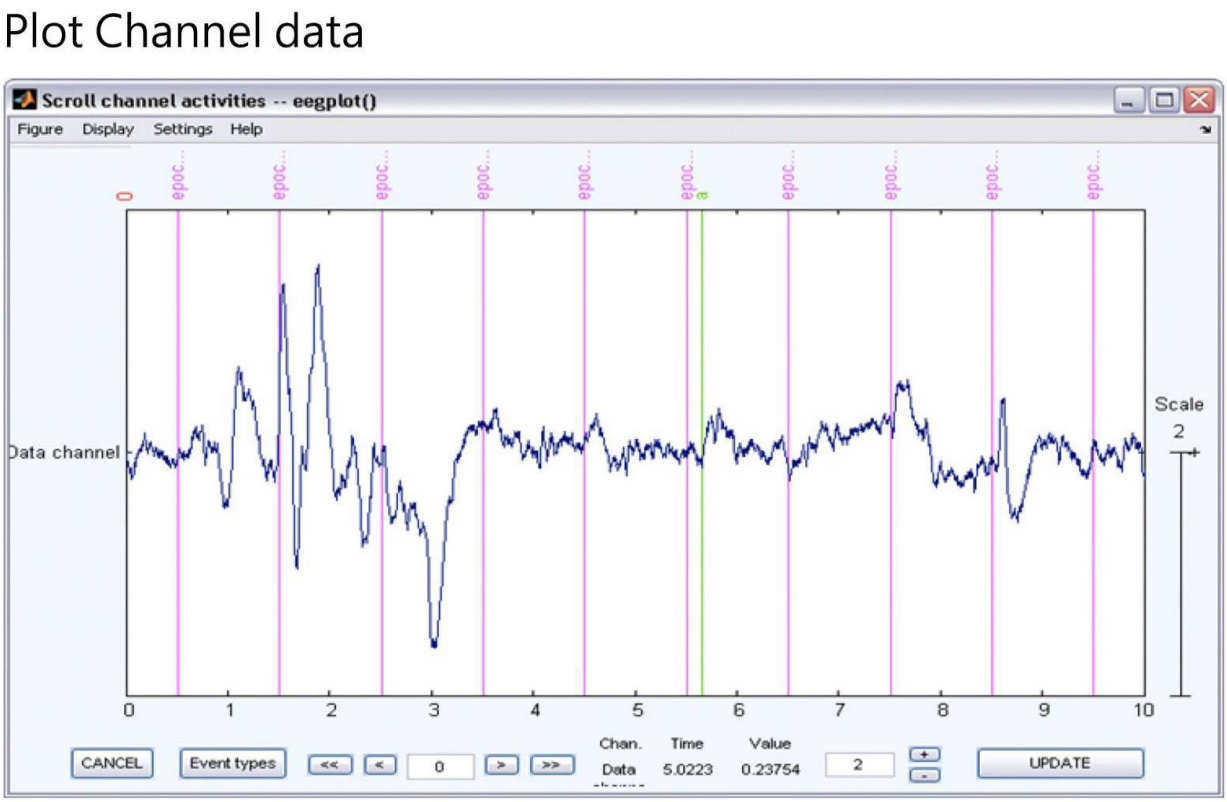

FIGURE 2. Sampling the raw data signal of one user.

electrodes, which are put in the Fp1 (left and frontal lobe) of the human forehead. According to [45], [46], the frontal lobe of the brain is in charge of motor control (dizziness, vertigo, and fatigue), cognitive (Concentration, problem-solving, and planning), and speech. We recorded for around ten minutes until the user notified us that they have motion sickness. The VR environment we used is a roller coaster simulation, which feels like riding a roller coaster.

A sample of the raw data signal from a user is shown in Figure 2. We applied the 512Hz digital sampling at one second intervals to filter the analog data to form a potential electrical signal. Analog data can be changed into a digital format using the Fast Fourier Transform (FFT) [47]. A Fourier series decomposes a periodic signal x(t) regarding an infinite sum of sin and cosines [48]. The formula is shown by equation (1).

$$x(t) = \frac{a_0}{2} + \sum_{k=1}^{\infty}(a_n cos(\omega kt) + b_n sin(\omega kt)) \tag{1}$$

where $x(t)$ is the produced raw data signal. $x(t)$ can be integrated on an interval $[0, T]$. The signal is periodic with a period of T where t is a time variable. ω is an angular frequency and a_0, a_n, and b_n are Fourier coefficients. The parameters we use to calculate the Fourier transform are inspired by [48] and are shown in equation (2).

$$x(t) = \sum_{k=-\infty}^{k=\infty} c_n . e^{j\omega kt} \tag{2}$$

where the coefficient c_n is obtained from equation (3):

$$c_n = \frac{1}{T}\int_0^T x(t)e^{-j\omega kt}dt \tag{3}$$

The generalization of the Fourier series can be used for infinite domains in the form of a Continuous Fourier Transform (CFT). This function is used to transform the signal between the time and frequency domain. The CFT function is shown by equation (4).

$$F(\xi) = \int_{-\infty}^{\infty} x(t)e^{2\pi j\xi}dt \tag{4}$$

The transformation of the signals between the time and frequency domains is handled by the inverse function of the CFT. Equation (5) shows the inverse CFT function.

$$x(t) = \int_{-\infty}^{\infty} x(t)e^{2\pi j\xi}d\xi \tag{5}$$

When the signal is periodically in T, then the CFT can be represented exactly by Discrete Fourier Transform (DFT). The frequency ξ is equal with $\frac{\omega}{2\pi}$ cycles per second or Hertz (Hz, KHz, MHz, GHz, etc.), instead of ω in radians per second. The function of the Fourier Transform is to transform the sequence of N complex numbers from the time domain $(x_0, x_1, x_2, \ldots, x_{N-1})$ into an $N-periodic$ sequence $X_0, X_1, X_2, \ldots, X_{N-1}$ (the list of the coefficients of a finite combination of complex sinusoids, ordered by their frequencies). The DFT function is shown in equation (6).

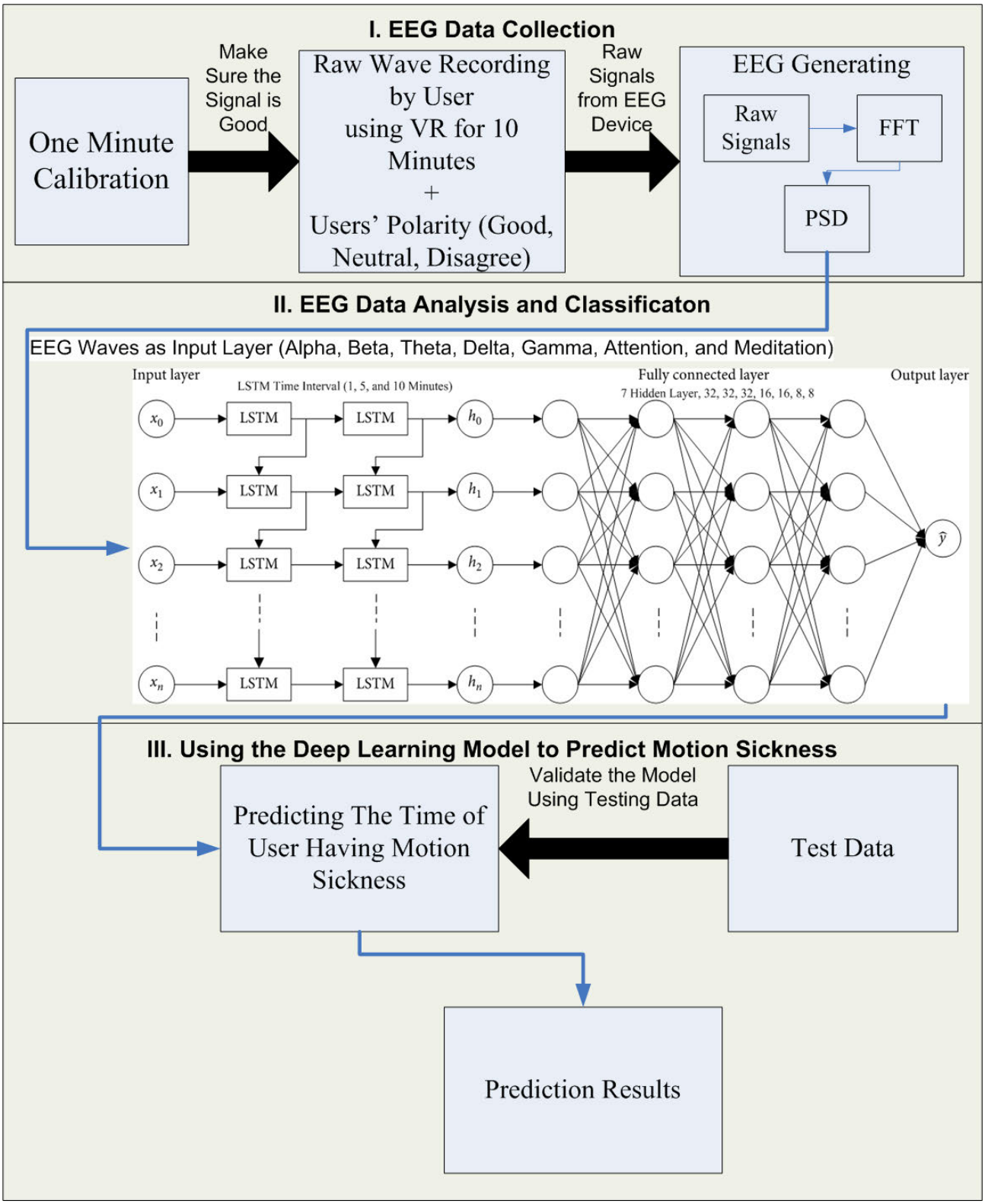

FIGURE 3. The system architecture.

Figure 4 shows the PSD results for the user. We developed the system to record the results based on the voltage and frequency spectrum. The generated waves are shown in the using line chart. The bar-chart is the PSD sampling showing the user's raw wave that has been processed. The system also records attention and meditation that is shown by the line

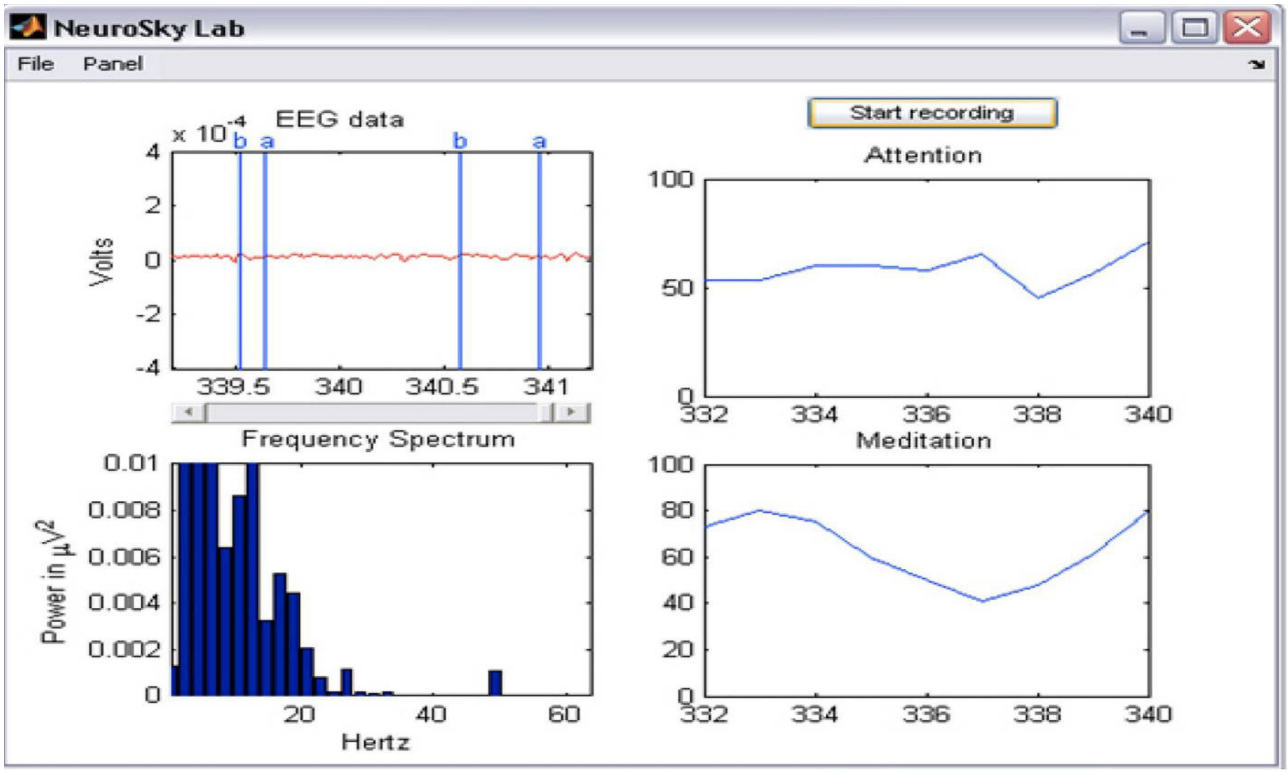

FIGURE 4. EEG, attention, and meditation recording interface via PSD methods.

chart on the right-side.

$$X_k = \sum_{n=0}^{N-1} x_n e^{-\frac{j2\pi kn}{N}} \tag{6}$$

A random signal usually has finite average power and is characterized by an average spectral density as shown in equation (7).

$$PSD_f(w) = \lim_{T\to\infty} \frac{|F_{X_T}(\omega)^2|}{2T} \tag{7}$$

$|F_{X_T}|$ is the FFT function for the signal output from the user, and T is the total time of the input signal. W is a set of brainwave bands: Alpha, Beta, Theta, Delta, and Gamma. Power Spectral Density (PSD) is derived from the Fourier transform where the power present in the signal is a function of frequency, per unit frequency. The signal is distributed with the frequency. ω represents angular frequency.

In the deep learning model's training model phase, the dataset consists of a set of users, $U = \{u_1, u_2, \ldots, u_i\}$ and a set of brainwaves, $Bw = \{bw_1, bw_2, \ldots, bw_j\}$ where i is the number of users and j is the number of brainwaves. The condition for each brainwave or product bw_j with user u_i is expressed by Condition $C = [U, Bw]_{i\times j}$. The matrix C denotes the condition of user u_i with brainwaves or product bu_j where i is an index of the user, and j is an index of brainwaves. The elements of C are a binary to represent the condition of the user. Zero represents normal condition and 1 represents motion sickness condition.

In this paper, we represent the condition value by using a binary value as the output in the system model. This research proposes an alternative approach to calculate user motion sickness using brainwaves. For each band of brainwaves, we obtain a set of targets T, where $T = \{t_1, 1, t_1, 2, \ldots, t_(j, i)\}$, $t_{j,i}$ represents brainwaves bw_j which is obtained from user u_i. Table 2 indicates the relationship between users and brainwaves for the condition target (Motion Sickness or Normal Condition), and Table 3 indicates the relationship between brainwaves and users for measurements.

TABLE 2. Users - Brainwaves relationship for motion sickness.

U/Bw	u_1	u_2	...	u_m
Bw_1	N	N	...	N
Bw_2	N	N	...	N
...	...	...	...	...
Bw_n	M	M	...	M
$*M : MotionSickness$				
$*N : Normal$				

TABLE 3. Users - Brainwaves relationship for measurements.

U/Bw	u_1	u_2	...	u_m
Bw_1	$t_{1,1}$	$t_{2,1}$	...	$t_{m,1}$
Bw_2	$t_{1,2}$	$t_{2,2}$	...	$t_{m,2}$
...	...	...	...	...
Bw_n	$t_{1,n}$	$t_{2,n}$	...	$t_{m,n}$

The CS point is calculated by summing the user's alpha wave plus theta wave and dividing by their beta wave. From equation (8), each user has a CS point value.

TABLE 4. Description of the CS point of the output layer.

Value of The CS Point	Level	Status of the User
81-100	Severe Sickness	The user's feeling of sickness is very high. The user is becoming severely tired. The user is likely to terminate VR.
61-80	Moderate Sickness	When the sickness value falls between 61 and 80, the user has begun to feel symptoms of CS.
41-60	Normal	The user is in normal condition and likely to continue using VR
21-40	Light Excited	When the sickness value is between 21 and 40, the user is likely in a state of low excitement, and the response to events is normal.
01-20	Excited	At this level, the user is in an excited state and cannot easily develop CS within a short time.

Combined with deep learning, this value is classified into sickness levels (Table 4). Table 4 uses the SSQ sickness range from [49], [50]. Reference [49] collected 47 symptom items used in VR research. They added an item for vision discomfort to increase the number of items related to vision quality and decided to remove the item "discomfort from eyes" because they felt that it was ambiguous. This left 23 symptom items: 12 non-ocular and 11 ocular. They created a seven-option response scale (scored 0-6) with four descriptive labels ("none" (0), "slight" (1, 2),"moderate" (3, 4), and "severe" (5, 6). Based on [49], we classified the sickness levels as shown in Table 4.

The sickness index for each user affects the sickness level during the calculation. The Attention and Meditation (*Att* and *Med*) are obtained from Neurosky's algorithm and are used to detect the attention and meditation state of the user. *Att* indicates the intensity of a user's level of mental "focus" or "attention". *Med* indicates the level of a user's mental "calmness" or "relaxation" [23]. If the *Att* value is greater than or equal to the *Med* value, then the sickness index value will be added to the value of CS_p. However, if the Med value exceeds the *Att* value, then the sickness index value will subtract the value of CS_p.

$$CS_p = \frac{\sum \alpha + \sum \theta}{\sum \beta} \tag{8}$$

The system generates brainwave vectors for all user brainwave targets which are represented as $Ve = [Ve(u, bw)]_{k,l}$, where k is the dimension of vector and l is the total number of user measurement targets u for brainwave bw. Matrix Ve is the vector representing the brainwave targets of user u_j to brainwave bu_i. We use the vectors as the input for our deep learning model. Figure 5 shows the preview of the input vector Ve.

Figure 6 shows the deep learning system architecture for detecting motion sickness from users' brainwaves. The model consists of 7 hidden layers with the first three hidden layers consisting of 32 nodes, the second two hidden layers consisting of 16 nodes, and the third two hidden layers consisting of 8 nodes. The input nodes are the brainwave frequency values of the alpha, beta, delta, theta and gamma frequencies. The output layer consists of 1 node only, which classifies whether the output belongs to a sick or normal state. The equation for the LSTM with a forget gate is shown by equation (9).

$$\begin{aligned} f_t &= \sigma_g(W_f x_t + U_f h_{t-1} + b_f) \\ i_t &= \sigma_g(W_i x_t + U_i h_{t-1} + b_i) \\ o_t &= \sigma_g(W_o x_t + U_o h_{t-1} + b_o) \\ \bar{c}_t &= \sigma_g(W_c x_t + U_c h_{t-1} + b_c) \\ c_t &= f_t \cdot c_{t-1} + i_t \cdot \bar{c}_t \\ h_t &= o_t \cdot \sigma_h(c_t) \end{aligned} \tag{9}$$

where c represents memory cell, i represent the input gate, o represent the output gate, and f represent the forget gate of the memory cell ct. $\bar{c}$ represents the candidates value of the cell state, and h represent the hidden layer output.

Long Short Term Memory (LSTM) is an effective deep learning algorithm used to predict a Time Series. A common LSTM model is composed of a cell, an input gate, an output gate, and a forget gate. LSTM performs well in time series data prediction because of its capability to "remember" while "forgetting" unimportant information. LSTM is designed to avoid the long-term dependency problem. All LSTM models take the form of a chain of repeating modules of a neural network. In this paper, the input LSTM layer is the feature vector Ve for each user. In the LSTM input nodes are represented by x_t, meaning that the system simply inputs all Ve values into x_t. The next step in the LSTM is to decide what information is will be discarded from the cell state.

	A	B	C	D	E	F	G	H	I	J	K	L	M	N	O	P	Q	R	S	V2
1	V1	V2	V3	V4	V5	V6	V8	V10	V11	V12	V13	V14	V15	V16	V17	V18	V19	V20	V21	
2	0.666667	0.333333	1	0	0	0	0.333333	0	0	0	0	0	0	0	0	0	0	0	0	
3	0.333333	0	1	0	0	0	0	0	0	0	1	0	0	0	0	0	0	0.333333	0.333333	
4	0.333333	0	1	0	0.333333	0	0	0	0	0	0	0	0	0.333333	0	0	0	0	0	
5	1	0.333333	1	0.666667	0	1	1	0	0	0	0	0	0	0	0	0	0	0	0	
6	0.333333	0	0.333333	0.333333	0	0	0	0	0	0.333333	0.333333	0	0	0	0	0	0	0	0	
7	0.5	1	0	0	0	0	0.5	0	0	0	0.5	0	0	0.5	0	0	0	0	0	
8	0	1	0	1	0	0	0	0	0	1	0	0	0	0	0	0	0	1	0	
9	0	0.333333	1	0	0	0	0.666667	0	0	0	0.666667	0.666667	0	0	0	0	0	0.333333	0	
10	0.333333	0	0	0	0	0	0	0	0	0.333333	1	0	0	0	0	0	0	0	0	
11	1	1	1	0	0	0	0	0	0	0	1	1	0	0	0	0	0	0	0	
12	0.25	0.5	1	0.25	0	0	0	0	0	0.25	0.25	0.25	0	0	0	0	0	0	0	

FIGURE 5. The preview of input vector *Ve*.

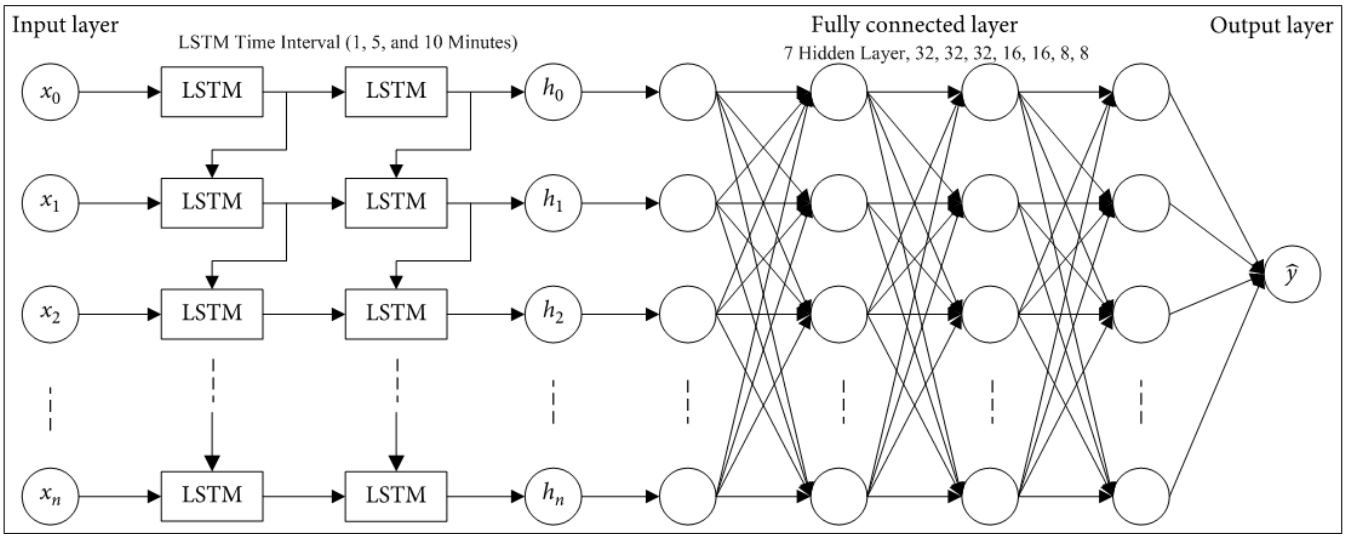

FIGURE 6. Deep learning architecture using LSTM and fully connected layer.

The decision is made by the forget gate layer f_t using a sigmoid function σ_g. The function looks at h_{t-1} and x_t, and outputs a number between 0 and 1 for each number in the cell state c_{t-1}. Output 1 represents retaining the information, and 0 represents discarding it.

The next step is to decide what information the system going to store in the cell state. The process also uses a sigmoid function σ_g which determines what value the system will update. Next, a candidate value $\bar{c}_t$ is created from the input layer and the candidates then added to the state. In this paper, the system wants to remember the waves of the new subject to the cell state, to replace the previous one, which the model forgets. After that, the system updates the c_t value by multiplying the forget gate layer f_t by c_{t-1} and adding the new candidates value c_t to it.

In the final step, the system must decide what the output is. The output is based on the system cell state with a filtered version. The output consists of two parts, the first is to applied the sigmoid function σ_g to decide what parts of the cell state the system will output. The second part puts the cell state into the tanh function σ_h and multiplies it by the output of the sigmoid function, so that the system only outputs the parts the user needs.

Table 5 shows the hyper-parameter setting, a summary of the deep learning model, and the dropout configuration. The model consists of 1 input layer, 1 LSTM layer, 7 hidden layers, and 1 output layer. The input layer consists of 10 nodes, and the type is dense, with a ReLU activation function. The LSTM layer consists of 32 nodes. The system uses the time-steps LSTM model. We applied 3 time-step configurations using 60, 300, and 600. In the full connected layer, the system consists of 7 hidden layers. The nodes of the hidden layers consist of 32, 32, 16, 16, 16, 8, and 8 nodes, respectively. The type is dense, with a RELU activation function. The output layer consists of 1 node with a sigmoid activation function. The system applies the l1 and l2 regularization functions, and the RMSProp optimizer function.

TABLE 5. The configuration of the deep learning model.

Layer	Type	Nodes	Activation Function	Rate
Input Layer	Dense	10	RELU	-
LSTM Layer	lstm	32	tanh	-
Dropout_1	Dropout	32	-	0.5
Hidden Layer 1	Dense	32	RELU	-
Hidden Layer 2	Dense	32	RELU	-
Hidden Layer 3	Dense	16	RELU	-
Hidden Layer 4	Dense	16	RELU	-
Hidden Layer 5	Dense	16	RELU	-
Hidden Layer 6	Dense	8	RELU	-
Hidden Layer 7	Dense	8	RELU	-
Output Layer	Dense	1	Sigmoid	-

IV. DATASET AND TRAINING ENVIRONMENT

In this section, we will describe our data collection and the training environment of our system. The system uses the brainwaves dataset, which is collected from our experiment lab. The dataset consists of 130 individuals who have used VR. The brainwaves, delta, theta, low alpha, high alpha, low beta, high beta, low gamma, and high gamma, are collected during the experiments. The target labels are motion sickness and normal state value. Table 6 shows a preview of the users' brainwaves attributes collected by the system. In the dataset, the users are young people ranging from 6 to 23 years old, 65 males and 65 females. The duration of the brainwaves recorded is 10 minutes, with 1 minute used for calibration. The calibration process ensures the signal from the EEG device is recorded clearly in the database. The process simply permits the user to adapt to the use of the EEG device. We let the user use the device for 1 minute and record only the signal quality. The system records the signal quality and calculates the rate at which the EEG device returns a bad signal. The Neurosky EEG Device has a methodology to detect good and bad signals automatically. If the loss is more than 20% the system will signal that the user must re-calibrate the device. Thus, the total time the user spends in the VR world is 11 minutes. The VR world for the experiments includes

TABLE 6. Number of participants, mean age, and standard deviation in experiments.

Group	Male		Female		Total	
	N	M_age (SD)	N	M_age (SD)	N	M_age (SD)
People with Motion Sickness	25	20(1.42)	45	16(2.41)	70	18(1.91)
People without Motion Sickness	35	16(2.57)	20	15(1.73)	60	15(2.17)

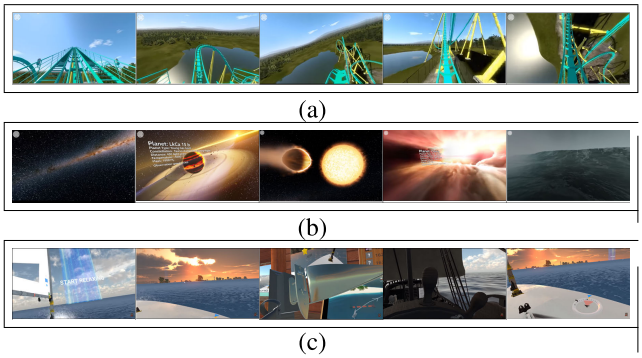

FIGURE 7. Preview of the VR environment sampling: (a) roller coaster VR; (b) space simulator; (c) Boat.

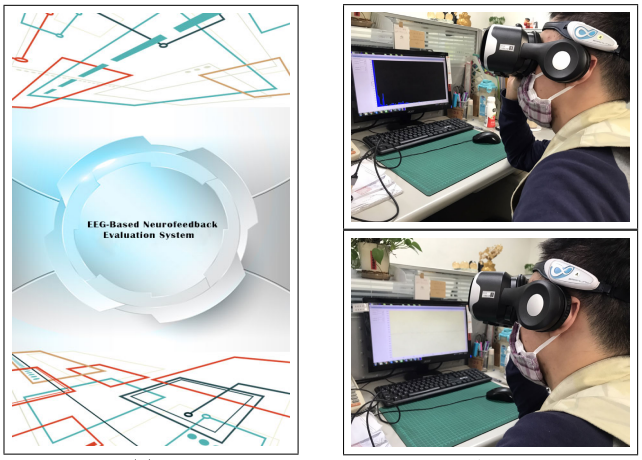

FIGURE 8. The experimental setup: (a) The main interface; (b) The user experiment.

a roller coaster, a space simulator, and a boating experience on the ocean. Figure 7 shows the sampling preview for each VR environment.

In this paper, the dataset will be divided into 70% for training the model, and 30% for testing. Validation data will be generated using 30% of the training data. We generate validation data in order to avoid training an over-fitting model. Ten minutes of the brainwaves will be recorded every second. We recorded 130 multiples of 600s of EEG data. Our dataset consists of a total of 78,000 records of brainwave signals, with 8 attributes for each instance. The sickness detection system contains 3 attributes and 2 attribute labels, motion sickness and normal state. The dataset also consists of 1 attribute of signal quality to check whether the instances which are recorded are good. The features from the dataset used in the deep learning model are EEG waves, including low alpha, high alpha, low beta, high beta, theta, delta, low gamma, and high gamma waves (8 nodes), sickness detection including attention (1 node), meditation (1 node), and CS_p (1 node). The 10 nodes form the input layer of the LSTM layer $X_t = \{x_0, x_1, \ldots, x_{10}\}$.

The experiments are conducted in a laboratory where in which users using VR headset device and Neurosky participants used VR headset devices and a Neurosky brainwaves headset. Figure 8 gives an illustrates the overview of the experiments we conduct and an example of an user was undergoing the described experiment using the VR headset and EEG tracking device. The training environment is run in core I7 CPU, with a GTX1080Ti NVidia Graphical Processing Unit (GPU), and the 32GB of RAM Memory is used.

V. EXPERIMENTS AND RESULTS

The system uses a grid search to tune the hyper-parameter. The system deep learning model's hyper-parameter configuration is as follows. The number of hidden layers is 7, with the number of nodes set to 32, 32, 32, 16, 16, 8, and 8 respectively. The activation function for each hidden layer is ReLU, the batch size is 100, epochs are 125, and the dropout rate is 0.5. We also implement l1 and l2 regularization, and the RMSProp optimizer. We use 3 combinations of time steps in the LSTM: 1, 5, and 10 minutes, to predict Motion Sickness.

The setting value of hyperparameters uses a grid search with different dimensions, learning rates, and activation function. We run the first ten iterations to get a preview of the best configuration. The accuracy and kappa metrics are used to measure the proposed hyper-parameter setting. We find that using layer c(32,32,16,16,16,8,8) with 5 learning rate returns the best accuracy value 0.339; using layer c(32,32,16,16,8,8) with learning rate 10 returns the second-best accuracy value with 0.334; and using layer c(32,32,16,16,8) with 5 learning rate returns the third-best accuracy value 0.326. From accuracy, the system chooses the settings accordingly.

A. RESULTS

Figure 9 shows the training phase loss from the system. It is clear that our model does not face over-fitting problems. The loss value is higher than the validation loss value, indicating that our model can predict the generalization of the problem well.

Figure 9(a) shows the training loss for LSTM with 60s time steps. The loss value converge after 30 iterations; the Mean Square Error (MSE) loss of the model can achieve 0.088. We can also find that the validation loss is below the loss value's line. When the validation loss is lower than the loss value, the model fits not only for the training data. Figure 9(b) shows the training loss for the LSTM with 300s

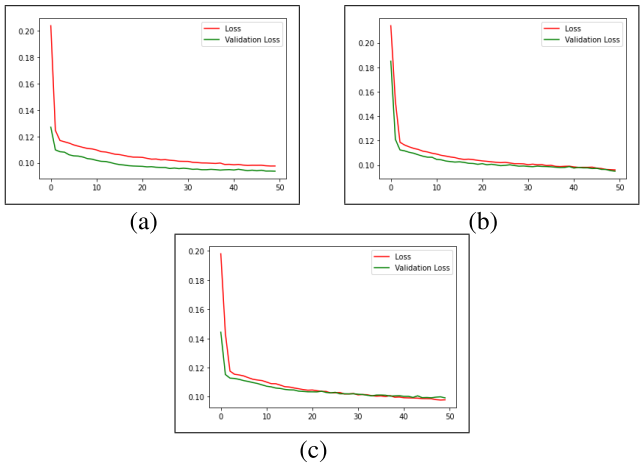

FIGURE 9. Deep learning training loss: (a) Loss for 1 minute predictor, (b) Loss for 5 minutes predictor, (c) Loss for 10 minutes predictor.

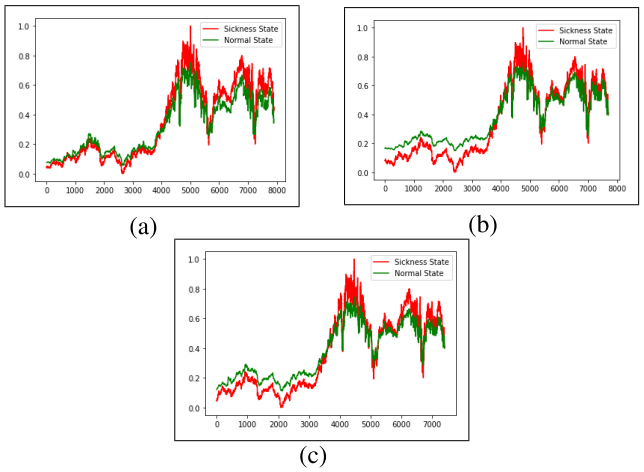

FIGURE 10. Deep learning training sickness predictor: (a.) Sickness prediction for 1 minute predictor, (b.) Sickness prediction for 5 minutes predictor, (c.) Sickness prediction for 10 minutes predictor.

time steps. The loss value converges after 40 iterations and the minimum MSE loss the model is achieved at 0.095. The loss value line will likely fall below the validation loss value line after 60 iterations, indicating that the training should stop at this iteration to prevent the model from over-fitting the data. Figure 9(c) shows the training loss for LSTM with 600s time steps. The loss value converges after 30 iterations, and will likely fall below the validation loss value after 40 iterations. The model can achieve the minimum MSE loss value at 0.101.

We compare the different time steps, as shown in Table 7. The best time step accuracy occurs with the 60s time steps, followed by the 300s time steps, and the 600s time steps. This means that predicting the next 60s will likely give better results than a longer time prediction. Table 7 confirms this. It is true that the shortest time prediction will give the best results, but the action to mitigate the problem also very short. For example, as we know that in the next 60s the user is predicted to experience motion sickness, and perhaps is already feeling symptoms. The feedback is already too late for the user to mitigate or avoid the symptoms. Even if the user reduces or stops using the VR, they likely will still feel a little bit of headache, nausea, and discomfort. The best notification feedback for the motion sickness is 5 minutes before it occurs. When the user terminates VR 5 minutes before the predictor notification, they are less likely to feel the symptoms yet can enjoy VR longer than with the 10 minutes notification.

TABLE 7. Comparison of results between time steps in dataset.

Time Steps(s)	MSE	MAE	Accuracy
60	0.088646	0.140032	83.94%
300	0.095044	0.139949	83.83%
600	0.101905	0.139872	83.92%

Figure 10 shows the predicted sickness state from the dataset. The predictor is divided into 1, 5, and 10 minutes. In the beginning, the green line is above the red line. This implies that the condition of normal state is higher than sickness state. Figure 10(a) shows the 1 minute predictor in every 10 minutes. We find that the red line rises above the green line after an individual uses the VR system for 40 minutes. This means our model predicts the onset of motion sickness symptoms. Figure 10(b) shows the 5 minutes predictor at 10 minute intervals. We find that the red line rises above the green line after 37 minutes, 3 minutes earlier than with the 1 minute predictor. Figure 10(c) shows the 10 minutes predictor at 10 minute intervals. We find that the red line rises above the green line after 35 minutes of using VR. The system predicts sickness earlier with longer time steps.

Table 8 shows the confusion matrix of the testing data. The system aims to predict the EEG pattern and decides whether the user has motion sickness. The testing data consists of 30,000 records of EEG patterns. The system predicts correctly normal conditions with 15,256 patterns and sickness conditions with 6,816 patterns. A false positive is an error that occurs when a system falsely concludes an effect exists, or when the system predicts incorrectly of a real class. Based on the confusion matrix, the system falsely predicts the real class with 3,088 patterns. For the research, it is impossible to know 100% certainty the true state of the world. Our system has around a 14% false-positive rate. According to [51], the false positive rate is ideally lower than 10%. If the false-positive rate value is lower than 15%, the user responses are categorized by suspicious, but not invalid. This is the limitation of our current research, as the false positive rate may come from an inconsistency respondent's report.

TABLE 8. The confusion matrix for testing data.

	Classes	
Target Data	Normal	Motion Sickness
Normal	15,256	3,088
Motion Sickness	4,840	6,816

B. COMPARISON WITH BASELINE METHODS

We also compare the results among with those of state-of-the-art methods. The model will be evaluated with the following baselines.

TABLE 9. Comparison of results for different algorithms (test phase).

Dataset	Methods	RMSE	MAE	Precision	Recall	F-Score
VR in Roller Coaster	MLP	0.30	0.18	71.31	71.62	0.71
	LibSVM	0.38	0.15	62.58	82.03	0.71
	CNN	0.31	0.14	73.81	80.47	0.77
	Proposed Method	**0.30**	**0.14**	**82.83**	**91.61**	**0.87**
VR in Space Simulator	MLP	0.34	0.23	63.84	54.84	0.59
	LibSVM	0.42	0.17	65.63	44.44	0.53
	CNN	0.29	0.16	65.87	**64.15**	**0.65**
	Proposed Method	**0.26**	**0.10**	**75.85**	53.87	0.63
VR in Sea Boat	MLP	0.35	0.24	48.00	**28.80**	0.36
	LibSVM	0.44	**0.19**	**60.02**	27.80	**0.38**
	CNN	0.35	0.21	55.04	19.68	0.29
	Proposed Method	**0.34**	0.20	59.23	26.90	0.37

- Support vector machine: we use the libsvm, which classifies data based on a linear kernel. Since the training process permits sparse data, the training dataset comprises non-zero values. The parameter setting of the training kernel is as follows. The batch size is 100, cacheSize is 40, cost is 1, degree is 3, and the kernel type is radial basis function.
- Multi layer perceptron: We use the Weka library MLP, a sigmoid function, a squared error function, and a mean absolute error function for the evaluation of the classification approaches. The parameter setting of the training is as follows. The batch size is 100 and consists of one hidden layer, the learning rate is 0.3, momentum is 0.2, and training epochs is 500.
- Convolution neural network: We employ Weka deeplearning4j and, use a deep neural network with hyper-parameter settings as follows. The batch size is 100, the epochs is 100, the optimizer is Adam, the bias updater is SGD, we implement l1 and l2 regularization, and the hidden layers consist of 7 hidden layers, with configuration nodes 32, 32, 16, 16, 16, 8, and 8.

Table 9 shows the comparison results between these algorithms. We separate the results based on the experimental data. First, we collect the brainwave data using VR. From the table, we find that our model outperforms the other models. We use Root Mean Square Error (RMSE) loss, Mean Average Error (MAE) loss, Accuracy, and F-measure as performance metrics. For the VR Roller Coaster, our model obtains the best RMSE loss at 0.3, followed by the Convolution Neural Network (CNN) RMSE loss at 0.38, Multi Layer Perceptron (MLP) RMSE (0.31), and the LibSVM RMSE (0.38). For the MAE loss value, our model has the best loss value, 0.14, followed by the CNN MAE at 0.14, the LibSVM loss value at 0.15, and MLP at 0.18. We also examine other metrics. In accuracy metrics, our model has the best accuracy value with 82.83%, followed by CNN at 73.13%. MLP at 71.31% and LibSVM at 62.58%. To accommodate the recall value, we also compare the F-measure across these the algorithms. Our model also has the best F-measure value, 0.87, followed by CNN at 0.77, MLP model at 0.71, and LibSVM at 0.71.

In the brainwave VR in Space Simulator, our model has the best RMSE loss at 0.26, followed by CNN at 0.29, MLP at 0.34, and LibSVM at 0.42. For the MAE loss value, our model again has the best loss value at 0.10, followed by CNN at 0.16, LibSVM at 0.17, and MLP at 0.23. In accuracy metrics, our model has an accuracy of, 75.85%, followed by CNN at 65.87%, LibSVM at 65.63%, and MLP at 63.84%. To accommodate the recall value, we also compare the F-measure across these the algorithms. CNN has the best value at 0.65. Our proposed method is second at 0.63, followed by MLP at 0.59 and LibSVM at 0.53.

In the Boat VR, our model has the best RMSE loss at 0.34, followed by CNN at 0.35, MLP at 0.35 and LibSVM at 0.44. LibSVM has the best MAE loss value at 0.19, while our proposed method is second at 0.20, followed by CNN at 0.21, and MLP at 0.24. On the accuracy metric, LibSVM has the best value at 60.02, followed by our proposed method at 59.23, CNN at 55.04, and MLP at 48.00. To accommodate the recall value, LibSVM has the best f-score at 0.38, followed by our proposed method at 0.37, MLP at 0.36, and CNN at 0.29. In this dataset, our proposed method does not obtain the best values, but the differences are minor. It is also interesting to dig deeper into whether this seasickness is related to subjective feelings. Boating is a common experience and users may be more likely accept this sensation more easily than riding a roller coaster or moving in the space simulator, which are less common experiences. The smaller RMSE means the case has small variance in errors. The MAE is steady and RMSE increases as the variance associated with the frequency distribution of error magnitudes also increases. Our model better at learning phase with small outliers where the data more converge to the class.

VI. CONCLUSIONS

We propose a brainwave EEG for application to VR to predict motion sickness using a deep learning training model. Our experimental results show that our model outperforms all traditional models in loss values, accuracy, and F-measure metrics for the VR Roller Coaster. In other datasets, our model also performs well compared to other methods. Our model can achieve 82.83% accuracy from the dataset. We also found that 5 minute time steps to predict the motion sickness is the most useful configuration.

In the future, we will consider the subjective feeling of the event environment. Our results show that the boating environment results in a lower accuracy than the roller coaster and

space simulator. It will be interesting to explore more deeply into whether simulations of the real world and commonly experienced events are related to the experience of motion sickness when using VR.

ACKNOWLEDGMENT

The authors would like to thank Sheng Hong Precision Technology Co., Ltd., for providing the dataset brainwave using VR environment, and the Chaoyang University of Technology for providing the experiment environment.

REFERENCES

[1] T. A. Mikropoulos, "Brain activity on navigation in virtual environments," *J. Educ. Comput. Res.*, vol. 24, no. 1, pp. 1–12, Jan. 2001, doi: 10.2190/D1W3-Y15D-4UDW-L6C9.

[2] M. W. Krueger, T. Gionfriddo, and K. Hinrichsen, "VIDEOPLACE—An artificial reality," *SIGCHI Bull.*, vol. 16, no. 4, p. 35–40, Apr. 1985. [Online]. Available: https://doi.org/10.1145/1165385.317463

[3] S. Jones, "Towards a philosophy of virtual reality: Issues implicit in 'Consciousness Reframed,"' *Leonardo*, vol. 33, no. 2, pp. 125–132, Apr. 2000, doi: 10.1162/002409400552388.

[4] J. J. LaViola, "A discussion of cybersickness in virtual environments," *ACM SIGCHI Bull.*, vol. 32, no. 1, p. 47–56, Jan. 2000, doi: 10.1145/333329.333344.

[5] O. Merhi, E. Faugloire, M. Flanagan, and T. A. Stoffregen, "Motion sickness, console video games, and head-mounted displays," *Hum. Factors: J. Hum. Factors Ergonom. Soc.*, vol. 49, no. 5, pp. 920–934, Oct. 2007, doi: 10.1518/001872007X230262.

[6] A. C. P. de França and M. M. Soares, "Review of virtual reality technology: An ergonomic approach and current challenges," in *Advances in Ergonomics in Design*, F. Rebelo and M. Soares, Eds. Cham, Switzerland: Springer, 2018, pp. 52–61.

[7] S. Palmisano, R. Mursic, and J. Kim, "Vection and cybersickness generated by head-and-display motion in the oculus rift," *Displays*, vol. 46, pp. 1–8, Jan. 2017. [Online]. Available: http://www.sciencedirect.com/science/article/pii/S0141938216300713

[8] P. Kourtesis, S. Collina, L. A. A. Doumas, and S. E. MacPherson, "Technological competence is a pre-condition for effective implementation of virtual reality head mounted displays in human neuroscience: A technological review and meta-analysis," *Frontiers Hum. Neurosci.*, vol. 13, p. 342, Oct. 2019. [Online]. Available: https://www.frontiersin.org/article/10.3389/fnhum.2019.00342

[9] C. Tremmel, C. Herff, T. Sato, K. Rechowicz, Y. Yamani, and D. J. Krusienski, "Estimating cognitive workload in an interactive virtual reality environment using EEG," *Frontiers Hum. Neurosci.*, vol. 13, p. 401, Nov. 2019. [Online]. Available: https://www.frontiersin.org/article/10.3389/fnhum.2019.00401

[10] J. Tromp, D. Peeters, A. S. Meyer, and P. Hagoort, "The combined use of virtual reality and EEG to study language processing in naturalistic environments," in *Behavior Research Methods*. Cham, Switzerland: Springer, 2018.

[11] B. Rey, A. Rodríguez, and M. A. Raya, "Using portable EEG devices to evaluate emotional regulation strategies during Virtual Reality exposure," *Stud. health Technol. Informat.*, vol. 181, pp. 223–227, Sep. 2012.

[12] S. R. Carvalho, I. C. Filho, D. O. D. Resende, A. C. Siravenha, C. R. B. De Souza, H. Debarba, B. D. Gomes, and R. Boulic, "A deep learning approach for classification of reaching targets from EEG images," in *Proc. 30th SIBGRAPI Conf. Graph., Patterns Images (SIBGRAPI)*, Oct. 2017, pp. 178–184.

[13] A. Gomaa, M. M. Abdelwahab, M. Abo-Zahhad, T. Minematsu, and R.-I. Taniguchi, "Robust vehicle detection and counting algorithm employing a convolution neural network and optical flow," *Sensors*, vol. 19, no. 20, p. 4588, Oct. 2019.

[14] A. Gomaa, M. M. Abdelwahab, and M. Abo-Zahhad, "Real-time algorithm for simultaneous vehicle detection and tracking in aerial view videos," in *Proc. IEEE 61st Int. Midwest Symp. Circuits Syst. (MWSCAS)*, Aug. 2018, pp. 222–225.

[15] R. Thiyagarajan, C. Curro, and S. Keene, "A learned embedding space for EEG signal clustering," in *Proc. IEEE Signal Process. Med. Biol. Symp. (SPMB)*, Dec. 2017, pp. 1–4.

[16] Hendry and R.-C. Chen, "Automatic license plate recognition via sliding-window darknet-YOLO deep learning," *Image Vis. Comput.*, vol. 87, pp. 47–56, Jul. 2019. [Online]. Available: http://www.sciencedirect.com/science/article/pii/S0262885619300575

[17] S. Hell and V. Argyriou, "Machine learning architectures to predict motion sickness using a virtual reality rollercoaster simulation tool," in *Proc. IEEE Int. Conf. Artif. Intell. Virtual Reality (AIVR)*, Dec. 2018, pp. 153–156.

[18] C.-L. Chen, C.-Y. Liao, R.-C. Chen, Y.-W. Tang, and T.-F. Shih, "Bus drivers fatigue measurement based on monopolar EEG," in *Intelligent Information and Database Systems*, N. T. Nguyen, S. Tojo, L. M. Nguyen, and B. Trawiński, Eds. Cham, Switzerland: Springer, 2017, pp. 308–317.

[19] A. Lenartowicz and S. K. Loo, "Use of EEG to diagnose ADHD," *Current Psychiatry Rep.*, vol. 16, no. 11, p. 498, Nov. 2014.

[20] H. Berger, "Über das elektrenkephalogramm des menschen," *Archiv für Psychiatrie und Nervenkrankheiten*, vol. 94, no. 1, pp. 16–60, Dec. 1931. [Online]. Available: https://doi.org/10.1007/BF01835097

[21] J. Katona, I. Farkas, T. Ujbanyi, P. Dukan, and A. Kovari, "Evaluation of the NeuroSky MindFlex EEG headset brain waves data," in *Proc. IEEE 12th Int. Symp. Appl. Mach. Intell. Informat. (SAMI)*, Jan. 2014, pp. 91–94.

[22] D. Poltavski, "The use of single-electrode wireless EEG in biobehavioral investigations," in *Mobile Health Technologies*, vol. 1256. Cham, Switzerland: Springer, 2015, pp. 90–375.

[23] Neurosky. (2015). *Making sense of EEG Bands*. [Online]. Available: http://neurosky.com/2015/05/greek-alphabet-soup-making-sense-of-eeg-bands/

[24] J. Fell, G. Fernández, P. Klaver, C. E. Elger, and P. Fries, "Is synchronized neuronal gamma activity relevant for selective attention?" *Brain Res. Rev.*, vol. 42, no. 3, pp. 265–272, Jun. 2003.

[25] S. Weech, S. Kenny, and M. Barnett-Cowan, "Presence and cybersickness in virtual reality are negatively related: A review," *Frontiers Psychol.*, vol. 10, p. 158, Feb. 2019. [Online]. Available: https://www.frontiersin.org/article/10.3389/fpsyg.2019.00158

[26] K. M. Stanney, R. S. Kennedy, and J. M. Drexler, "Cybersickness is not simulator sickness," *Proc. Hum. Factors Ergonom. Soc. Annu. Meeting*, vol. 41, no. 2, pp. 1138–1142, Oct. 1997, doi: 10.1177/107118139704100292.

[27] G. De Leo, L. A. Diggs, E. Radici, and T. W. Mastaglio, "Measuring sense of presence and user characteristics to predict effective training in an online simulated virtual environment," *Simul. Healthcare: J. Soc. Simul. Healthcare*, vol. 9, no. 1, pp. 1–6, Feb. 2014.

[28] L. Rebenitsch and C. Owen, "Review on cybersickness in applications and visual displays," *Virtual Reality*, vol. 20, no. 2, pp. 101–125, Jun. 2016.

[29] M. McCauley and T. Sharkey, "Cybersickness: Perception of self-motion in virtual environments," *Presence*, vol. 1, pp. 311–318, Jan. 1992.

[30] J. D. Moss and E. R. Muth, "Characteristics of head-mounted displays and their effects on simulator sickness," *Hum. Factors: J. Hum. Factors Ergonom. Soc.*, vol. 53, no. 3, pp. 308–319, Jun. 2011, doi: 10.1177/0018720811405196.

[31] L. L. Arns and M. M. Cerney, "The relationship between age and incidence of cybersickness among immersive environment users," in *Proc. IEEE Virtual Reality Conf. (VR)*, Mar. 2005, pp. 267–268.

[32] P. Gamito, J. Oliveira, P. Santos, D. Morais, T. Saraiva, M. Pombal, and B. Mota, "Presence, immersion and cybersickness assessment through a test anxiety virtual environment," in *Annual Review of CyberTherapy and Telemedicine*. Brussels, Belgium: Virtual Reality Medical Institute, 2008, pp. 83–90.

[33] Y. Kim, H. Kim, E. Kim, H. Ko, and H.-T. Kim, "Characteristic changes in the physiological components of cybersickness," *Psychophysiology*, vol. 42, no. 5, pp. 25–616, Oct. 2005.

[34] M. S. Dennison, A. Z. Wisti, and M. D'Zmura, "Use of physiological signals to predict cybersickness," *Displays*, vol. 44, pp. 42–52, Sep. 2016. [Online]. Available: http://www.sciencedirect.com/science/article/pii/S0141938216301081

[35] E. Nalivaiko, S. L. Davis, K. L. Blackmore, A. Vakulin, and K. V. Nesbitt, "Cybersickness provoked by head-mounted display affects cutaneous vascular tone, heart rate and reaction time," *Physiol. Behav.*, vol. 151, pp. 583–590, Nov. 2015. [Online]. Available: http://www.sciencedirect.com/science/article/pii/S0031938415300974

[36] J. F. Golding, "Phasic skin conductance activity and motion sickness," *Aviation, Space, Environ. Med.*, vol. 63, no. 3, pp. 71–165, 1992.

[37] A. M. Gavgani, K. V. Nesbitt, K. L. Blackmore, and E. Nalivaiko, "Profiling subjective symptoms and autonomic changes associated with cybersickness," *Autonomic Neurosci.*, vol. 203, pp. 41–50, Mar. 2017. [Online]. Available: http://www.sciencedirect.com/science/article/pii/S1566070216301096
[38] M. Pierre, S. Banerjee, A. Hoover, and E. Muth, "The effects of 0.2 Hz varying latency with 20–100 ms varying amplitude on simulator sickness in a helmet mounted display," *Displays*, vol. 36, pp. 1–8, Jan. 2015.
[39] C. J. Lin, H.-J. Chen, P.-Y. Cheng, and T.-L. Sun, "Effects of displays on visually controlled task performance in three-dimensional virtual reality environment," *Hum. Factors Ergonom. Manuf. Service Ind.*, vol. 25, no. 5, p. 523–533, Sep. 2015. [Online]. Available: https://doi.org/10.1002/hfm.20566
[40] R. S. Kennedy, N. E. Lane, K. S. Berbaum, and M. G. Lilienthal, "Simulator sickness questionnaire: An enhanced method for quantifying simulator sickness," *Int. J. Aviation Psychol.*, vol. 3, no. 3, pp. 203–220, 1993. [Online]. Available: https://doi.org/10.1207/s15327108ijap0303_3
[41] S. Nichols and H. Patel, "Health and safety implications of virtual reality: A review of empirical evidence," *Appl. Ergonom.*, vol. 33, no. 3, pp. 251–271, May 2002.
[42] B. Keshavarz and H. Hecht, "Validating an efficient method to quantify motion sickness," *Hum. Factors: J. Hum. Factors Ergonom. Soc.*, vol. 53, no. 4, pp. 415–426, Aug. 2011, doi: 10.1177/0018720811403736.
[43] B. Keshavarz, R. Saryazdi, J. L. Campos, and J. F. Golding, "Introducing the VIMSSQ: Measuring susceptibility to visually induced motion sickness," *Proc. Hum. Factors Ergonom. Soc. Annu. Meeting*, vol. 63, no. 1, pp. 2267–2271, Nov. 2019, doi: 10.1177/1071181319631216.
[44] H. K. Kim, J. Park, Y. Choi, and M. Choe, "Virtual reality sickness questionnaire (VRSQ): Motion sickness measurement index in a virtual reality environment," *Appl. Ergonom.*, vol. 69, pp. 66–73, May 2018. [Online]. Available: http://www.sciencedirect.com/science/article/pii/S000368701730282X
[45] S. Riggio, "Traumatic brain injury and its neurobehavioral sequelae," *Neurologic Clinics*, vol. 29, no. 1, pp. 35–47, Feb. 2011. [Online]. Available: http://www.sciencedirect.com/science/article/pii/S0733861910001350
[46] A. Obenaus, "Traumatic brain injury," in *Encyclopedia Mental Health*. London, U.K.: Nature Publishing Group, Dec. 2016.
[47] D. V. Poltavski, D. Biberdorf, and T. V. Petros, "Accommodative response and cortical activity during sustained attention," *Vis. Res.*, vol. 63, pp. 1–8, Jun. 2012.
[48] W. Sałabun, "Processing and spectral analysis of the raw EEG signal from the MindWave," *Przeglad Elektrotechniczny*, vol. 90, pp. 169–174, Feb. 2014.
[49] S. L. Ames, J. S. Wolffsohn, and N. A. Mcbrien, "The development of a symptom questionnaire for assessing virtual reality viewing using a head-mounted display," *Optometry Vis. Sci.*, vol. 82, no. 3, pp. 168–176, Mar. 2005.
[50] N. Dużmańska, P. Strojny, and A. Strojny, "Can simulator sickness be avoided? A review on temporal aspects of simulator sickness," *Frontiers Psychol.*, vol. 9, p. 2132, Nov. 2018. [Online]. Available: https://www.frontiersin.org/article/10.3389/fpsyg.2018.02132
[51] J. A. Holdnack, S. Millis, G. J. Larrabee, and G. L. Iverson, "Assessing performance validity with the ACS," in *WAIS-IV, WMS-IV, and ACS*, J. A. Holdnack, L. W. Drozdick, L. G. Weiss, and G. L. Iverson, Eds. San Diego, CA, USA: Academic, 2013, ch. 7, pp. 331–365. [Online]. Available: http://www.sciencedirect.com/science/article/pii/B9780123869340000079

CHUNG-YEN LIAO (Member, IEEE) received the master's degree from the Department of Information Engineering, Chaoyang University of Technology, Taichung, Taiwan, in 2016. He is currently pursuing the Ph.D. degree with the Graduate Institute of Informatics, Chaoyang University of Technology. He is currently working with Sheng Hong Precision Technology Company Ltd. His research interests include EEG and brainwaves implementation, machine learning, and artificial intelligence.

SHAO-KUO TAI received the Ph.D. degree in computer science from National Chung Hsing University. He has been working with Chunghwa Telecom Company Ltd., since 1990. He is currently an Assistant Professor with the Chaoyang University of Technology. His scientific research interests include the application of artificial intelligence in medicine, the deep reinforcement learning problems, and the computer science in biology and medicine.

RUNG-CHING CHEN (Member, IEEE) received the B.S. degree from the Department of Electrical Engineering, National Taiwan University of Science and Technology, Taipei, Taiwan, in 1987, the M.S. degree from the Institute of Computer Engineering, National Taiwan University of Science and Technology, in 1990, and the Ph.D. degree in computer science sessions from the Department of Applied Mathematics, National Chung Tsing University, in 1998. He was the Department Chair of information management with the Chaoyang University of Technology, from 2005 to 2007. He has served as the Dean of the Informatics College, CYUT, from 2007 to 2015. He was the Execution Director of the Institutional Research Office, CYUT, from 2015 to 2017. He has served as the President of the Taiwanese Association for Consumer Electronics, from 2012 to 2014. He was a Visiting Professor with the University of Central Florida, USA, and The University of Aizu, Japan, in 2012 and 2017, respectively. He is currently a Distinguished Professor with the Department of Information Management, Taichung, Taiwan. His research interests include network technology, domain ontology, pattern recognition and knowledge engineering, the IoT and data analysis, and applications of artificial intelligence. He has been a Fellow of IET, since July 2011.

HENDRY HENDRY was born in Negara, Bali, Indonesia, in 1983. He received the B.S. degree in information technology from the Technology School of Surabaya, in 2005, the M.S. degree in information technology from the Tenth of November Institute of Technology, Surabaya, in 2009, and the Ph.D. degree in information management from the Chaoyang University of Technology, in 2018. From 2012 to 2014, he was the Director of the Business and Technology Incubator, Satya Wacana Christian University, Central Java, Indonesia. He is currently a Lecturer with the Faculty of Information Technology, Satya Wacana Christian University. His research interests include domain ontology, recommendation systems, knowledge engineering, and applications of artificial intelligence.